

Improved Algorithm for FEM Analysis of MTL Problems

Ivica Jurić-Grgić, PhD¹; Rino Lucić, PhD¹; Ivan Krolo, MD¹

¹University of Split, Faculty of Electrical Engineering, Mechanical Engineering and Naval Architecture, R. Boskovicca 32, HR-21000 Split, Croatia



Introduction

The finite element method (FEM) is the usual procedure for solving ODEs or PDEs for boundary value problems of mathematical physics. In the case of a spatial-temporal problem defined by a PDE, it is necessary to get an algebraic equation system for each finite element.

Although the generalized trapezoidal rule (θ -method) is A-stable method, in some cases it can produce numerical oscillations and numerical diffusion of results. This is because there is no universal value of time integration parameter θ that can achieve accurate results in all cases. Instead of using θ -method when forming a finite element matrix, the accuracy of a numerical solution can be improved using Heun's method for the time integration.

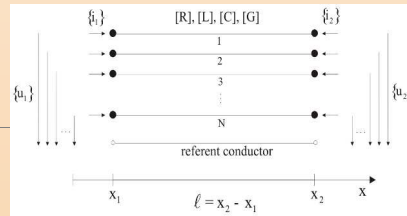


Figure 1. Multi-conductor transmission line finite element

MTL finite element – Heun's method

Propagation of traveling waves on MTL in the time-domain is governed by the Telegrapher Equations. Matrices $[R]$, $[L]$, $[C]$ and $[G]$ are frequency independent matrices of resistance, inductance, capacitance and conductance per-unit length, respectively (Figure 1). The voltage and current waves $\{u\}$, $\{i\}$ over the MTL finite element are approximated by a linear combination of linear interpolation (shape) functions. MTL finite element local system obtained by Heun's method can be written in the matrix form:

$$[A_1] \cdot \begin{Bmatrix} u_1 \\ u_2 \end{Bmatrix} + [B_1] \cdot \begin{Bmatrix} i_1 \\ i_2 \end{Bmatrix} = [E_1] \cdot \begin{Bmatrix} u_1 \\ u_2 \end{Bmatrix} + [F_1] \cdot \begin{Bmatrix} i_1 \\ i_2 \end{Bmatrix}$$

where:

$$[A_1] = \begin{bmatrix} [I] & [I] \\ -\frac{1}{\ell} \Delta t \cdot [C]^{-1} & -\frac{1}{\ell} \Delta t \cdot [C]^{-1} \end{bmatrix} \quad [B_1] = \begin{bmatrix} -\frac{1}{\ell} \Delta t \cdot [C]^{-1} & -\frac{1}{\ell} \Delta t \cdot [C]^{-1} \\ [I] & [I] \end{bmatrix}$$

$$[E_1] = \begin{bmatrix} ([I] - \Delta t \cdot [L]^{-1} [R] + \frac{1}{2} \Delta t^2 \cdot [L]^{-1} [R] [L]^{-1} [R]) & (-[I] + \Delta t \cdot [L]^{-1} [R] - \frac{1}{2} \Delta t^2 \cdot [L]^{-1} [R] [L]^{-1} [R]) \\ (\frac{2}{\ell} \Delta t \cdot [C]^{-1} - \frac{1}{\ell} \Delta t \cdot [C]^{-1} - \frac{1}{\ell} \Delta t^2 \cdot [C]^{-1} [G] [C]^{-1}) & (\frac{2}{\ell} \Delta t \cdot [C]^{-1} - \frac{1}{\ell} \Delta t \cdot [C]^{-1} - \frac{1}{\ell} \Delta t^2 \cdot [C]^{-1} [G] [C]^{-1}) \end{bmatrix}$$

$$[F_1] = \begin{bmatrix} (\frac{2}{\ell} \Delta t \cdot [L]^{-1} - \frac{1}{\ell} \Delta t \cdot [L]^{-1} - \frac{1}{\ell} \Delta t^2 \cdot [L]^{-1} [R] [L]^{-1}) & (-\frac{2}{\ell} \Delta t \cdot [L]^{-1} + \frac{1}{\ell} \Delta t \cdot [L]^{-1} + \frac{1}{\ell} \Delta t^2 \cdot [L]^{-1} [R] [L]^{-1}) \\ ([I] - \Delta t \cdot [C]^{-1} [G] + \frac{1}{2} \Delta t^2 \cdot [C]^{-1} [G] [C]^{-1}) & ([I] - \Delta t \cdot [C]^{-1} [G] + \frac{1}{2} \Delta t^2 \cdot [C]^{-1} [G] [C]^{-1}) \end{bmatrix}$$

The variables' vectors marked by "+" denote vectors at the end of the time interval, while variables' vectors without mark denote vectors at the beginning of the time interval.

Example 1 – Buried electrode

The example 1 presents propagation of an EM wave along a horizontal buried electrode. Burial depth of electrode is $h = 0.3$ m and radius of conductor is $a = 0.5$ cm. Buried conductor with length of 100 m has been modelled as a single transmission line with the following per-unit length parameters:

$R = 1.77 \cdot 10^{-4} \Omega/m$; $G = 2.94 \cdot 10^{-3} S/m$; $R = 1.42 \cdot 10^{-6} H/m$; $C = 1.64 \cdot 10^{-10} F/m$. The grounding electrode has been divided into 100 finite elements. The applied current waveform at the left end of the electrode is a step function with the amplitude of $I = 100$ kA and rise time of $T = 15.2 \cdot 10^{-8}$ s. At the right end of the electrode the current is set to zero (Figure 2). A computational time interval is $\Delta t = 1.52 \cdot 10^{-8}$ s.

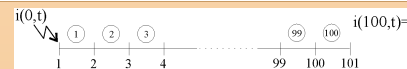


Figure 2. The finite element mesh and boundary conditions of the grounding electrode.

Figure 3 shows spatial distribution of voltage wave along buried electrode at $50 \cdot \Delta t$. Numerical solution obtained by Heun's method and the generalized trapezoidal rule (θ -method), for different values of a time integration parameter θ , are compared to the analytical solution obtained by the double Laplace transformation [7]. Since different values of θ yield different time-stepping schemes, all these schemes vary in accuracy. As it can be seen that numerical solution obtained by Heun's method yields highly accurate results while the generalized trapezoidal rule with $\theta = 0.66$ causes numerical damping of results. Furthermore, the generalized trapezoidal rule with $\theta = 0.5$ leads to numerical oscillations. Numerical experiments have shown that when using the generalized trapezoidal rule, in the case of a lossy line, optimal time integration parameter is $\theta = 0.66$ (Galerkin scheme).

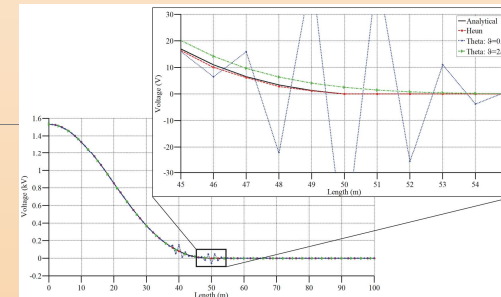


Figure 3. Spatial distribution of voltage wave along buried electrode at $50 \cdot \Delta t$.

Example 2 – Lossless MTL line

The following numerical example demonstrates the propagation of electromagnetic wave along simple 49.17-meter-long MTL, which is discretized into three MTL finite elements (Figure 4). In this example the conductor '2' of MTL has been grounded at the both sides (homogeneous Dirichlet boundary condition). The right end of the conductor '1' is open (the current at the boundary node is set to zero, homogeneous Neumann boundary condition) while on its left end the voltage wave is imposed (non homogeneous Dirichlet boundary condition).

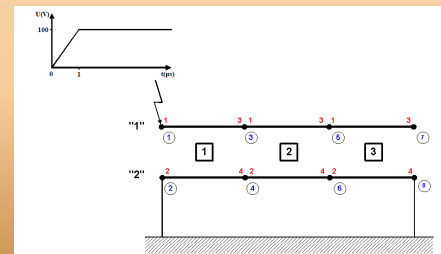


Figure 4. A two-conductor transmission line above reference plane.

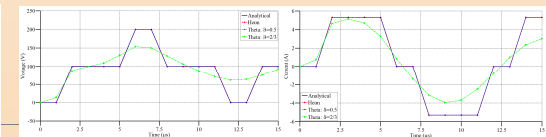


Figure 5. The voltage wave propagation at global node 3.

Figure 6. The current wave propagation at global node 3.

The applied voltage wave at the left end of conductor '1' is a step function with rise time of $T = 10^{-6}$ s. The numerical values of per-unit length matrices are:

$$[L] = \begin{bmatrix} 1.532 & 0.766 \\ 0.766 & 1.532 \end{bmatrix} \mu H/m \quad [R] = [0] \quad [C] = \begin{bmatrix} 3.12 & -1.56 \\ -1.56 & 3.12 \end{bmatrix} nF/m \quad [G] = [0]$$

Numerical experiments have shown that when using the generalized trapezoidal rule, in the case of a lossless MTL, optimal time integration parameter is no longer $\theta = 0.66$, as it was in the previous case. In the case of a lossless MTL line, optimal time integration parameter is $\theta = 0.5$ (Crank-Nicolson scheme). This is because there is no universal value of time integration parameter θ that can achieve accurate results in all cases. When using the generalized trapezoidal rule, usual way to find an optimal value of time integration parameter θ for particular TL problem are numerical experiments. Numerical solutions obtained by Heun's method and the generalized trapezoidal rule for $\theta = 0.5$ agrees with the analytical solution, while in a case of the generalized trapezoidal rule for $\theta = 0.66$, we have deviation of results (Figure 5 and 6).

Conclusions

In this paper an improved time integration scheme for time dependent FEM analysis of MTL problems was presented. Numerical solutions obtained using Heun's method and using the generalized trapezoidal rule for different values of a time integration parameter θ are compared to analytical solution. It has been shown that Heun's method yields the results with much higher accuracy comparing to results obtained by generalized trapezoidal rule (θ -method) with the approximately equal computational time. In some cases where the generalized trapezoidal rule is used, the choice of the numerical integration parameter (θ) generates numerical oscillations and/or numerical damping of results. Using the proposed approach, these unwanted consequences are avoided.

References

[1] O. C. Zienkiewicz and R. L. Taylor, The Finite Element Method, vol. 1, McGraw-Hill: London, UK, 1989.
 [2] O. C. Zienkiewicz and K. Morgan, Finite Element and Approximation, John Wiley & Sons: New York, USA, 1983.
 [3] R. Lucić, I. Jurić-Grgić and M. Kurtović, "Time domain finite element method analysis of multi-conductor transmission lines," Eur. Trans. Elect. Power, vol. 20, no. 6, 2010, pp. 822-832.

[4] I. Jurić-Grgić, R. Lucić and A. Bernardić, "Transient analysis of coupled non-uniform transmission line using finite element method," Int. J. Circ. Theor. Appl. vol. 43, no. 9, 2015, pp. 1167-1174.
 [5] S. C. Chapra and R. C. Canale, Numerical Methods for Engineers (7th Edition), McGraw-Hill: New York, USA, 2015
 [6] E. D. Sunde, Earth Conduction Effects in Transmission Systems, D. Van Nostrand Company: New York, USA, 1949.
 [7] R. Velazquez and D. Mukhedkar, "Analytical Modelling of grounding electrodes transient behavior," IEEE Trans. Power App. Syst., vol. PAS-103, no. 6, 1984, pp. 1314-1322.

